



**QUEEN'S  
UNIVERSITY  
BELFAST**

## Producing carbon nanotubes from thermochemical conversion of waste plastics using Ni/ceramic based catalyst

Liu, X., Shen, B., Wu, Z., Parlett, C. M. A., Han, Z., George, A., Yuan, P., Patel, D., & Wu, C. (2018). Producing carbon nanotubes from thermochemical conversion of waste plastics using Ni/ceramic based catalyst. *Chemical Engineering Science*, 192, 882-891. <https://doi.org/10.1016/j.ces.2018.07.047>

**Published in:**  
Chemical Engineering Science

**Document Version:**  
Peer reviewed version

**Queen's University Belfast - Research Portal:**  
[Link to publication record in Queen's University Belfast Research Portal](#)

### **Publisher rights**

Copyright 2018 Elsevier.

This manuscript is distributed under a Creative Commons Attribution-NonCommercial-NoDerivs License (<https://creativecommons.org/licenses/by-nc-nd/4.0/>), which permits distribution and reproduction for non-commercial purposes, provided the author and source are cited.

### **General rights**

Copyright for the publications made accessible via the Queen's University Belfast Research Portal is retained by the author(s) and / or other copyright owners and it is a condition of accessing these publications that users recognise and abide by the legal requirements associated with these rights.

### **Take down policy**

The Research Portal is Queen's institutional repository that provides access to Queen's research output. Every effort has been made to ensure that content in the Research Portal does not infringe any person's rights, or applicable UK laws. If you discover content in the Research Portal that you believe breaches copyright or violates any law, please contact [openaccess@qub.ac.uk](mailto:openaccess@qub.ac.uk).

### **Open Access**

This research has been made openly available by Queen's academics and its Open Research team. We would love to hear how access to this research benefits you. – Share your feedback with us: <http://go.qub.ac.uk/oa-feedback>

# 1           **Producing carbon nanotubes from thermochemical conversion of** 2           **waste plastics using Ni/ceramic based catalyst**

3           Xiaotong Liu<sup>a</sup>, Boxiong Shen<sup>b\*</sup>, Zhentao Wu<sup>c\*</sup>, Christopher M. A. Parlett<sup>d\*</sup>, Zhenan  
4           Han<sup>e</sup>, Adwek George<sup>b</sup>, Peng Yuan<sup>b</sup>, Dipesh Patel<sup>a</sup>, Chunfei Wu<sup>a,b\*</sup>

5           <sup>a</sup> School of Engineering and Computer Science, Faculty of Science and Engineering, University of  
6           Hull, Hull, HU6 7RX

7           <sup>b</sup> School of Energy and Environmental Engineering, Hebei University of Technology, Tianjin, China

8           <sup>c</sup> Aston Institute of Materials Research, School of Engineering and Applied Science, Aston University,  
9           Birmingham B4 7ET, UK

10           <sup>d</sup> European Bioenergy Research Institute, Aston University, Birmingham, B4 7ET, UK

11           <sup>e</sup> Wuhan Optics Valley Environmental Technology Co., Ltd, Wuhan City, China 430074

12           Corresponding authors: Tel: +44 (0) 1482466464, Email: c.wu@hull.ac.uk; Tel: +86 (0) 2260435784,  
13           E-mail: shenbx@hebut.edu.cn; Tel: +44 (0) 121204 3353, Email: z.wu7@aston.ac.uk; Tel: +44 (0)1212  
14           044100 c.parlett@aston.ac.uk)

## 16           **Abstract**

17           As the amount of waste plastic increases, thermo-chemical conversion of plastics  
18           provides an economic flexible and environmental friendly method to manage recycled  
19           plastics, and generate valuable materials, such as carbon nanotubes (CNTs). The choice  
20           of catalysts and reaction parameters are critical to improving the quantity and quality  
21           of CNTs production. In this study, a ceramic membrane catalyst (Ni/Al<sub>2</sub>O<sub>3</sub>) was studied  
22           to control the CNTs growth, with reaction parameters, including catalytic temperature  
23           and Ni content investigated. A fixed two-stage reactor was used for thermal pyrolysis  
24           of plastic waste, with the resulting CNTs characterized by various techniques including  
25           scanning electronic microscopy (SEM), transmitted electronic microscopy (TEM),  
26           temperature programm oxidation (TPO), and X-ray diffraction (XRD). It is observed  
27           that different loadings of Ni resulted in the formation of metal particles with various  
28           sizes, which in turn governs CNTs production with varying degrees of quantity and  
29           quality, with an optimal catalytic temperature at 700 °C.

30           *Keywords:* Plastics waste; Carbon nanotubes; ceramic membrane; Nickel; catalyst

## 31 **1. Introduction**

32 There was more than 4.3 million tonnes plastics waste generated in the UK in 2015 [1],  
33 the disposal of waste plastic causes environmental concerns. Therefore, careful  
34 management is needed to minimize the environmental impact of plastic waste. As waste  
35 plastic contains a high value of energy, recycle and recovery methods are encouraged  
36 compared to landfilling. Thermochemical recycling of waste plastics which converts  
37 plastics materials into other valuable materials, refers to an advanced technology  
38 process [2]. During this process, hydrogen-rich syngas is generated at high pyrolysis  
39 temperature ( $>800\text{ }^{\circ}\text{C}$ ) or gasification of waste plastics. For example, Erkiaga et al. [3]  
40 generated a syngas stream rich in  $\text{H}_2$  from pyrolysis of plastic waste (high density  
41 polyethylene) with Ni catalysts. Syngas has wide applications, including directly  
42 combusted for the production of heat and power, or conversion into liquid fuels through  
43 Fishcher-Tropsch process [4]. Recently, co-production of carbon nanotubes (CNTs)  
44 from pyrolysis or gasification of waste plastics has also attracted interest. CNTs were  
45 first introduced in 1952, and further inspired by Iijima [5, 6]. CNTs have extraordinary  
46 properties, including high mechanical strength, good electrical and thermal  
47 conductivity, and there promising potential applications. However, the high price  
48 ( $\sim\$85\text{-}95/\text{kg}$ ) has significantly prohibited the applications of CNTs [7]. Converting  
49 plastic waste to CNTs provides a promising alternative and economic flexible method  
50 to generate such high valuable material.

51 Chemical vapour deposition (CVD) is the current method of choice and widely utilised

52 to produce CNTs from plastics, due to its simplicity and low cost. This method used  
53 hydrocarbon gases as carbon sources and catalysts particles to nucleate the CNTs  
54 growth [8]. For example, Park et al. [9] optimized operation conditions with Ru-based  
55 catalysts from waste plastic, in order to decrease the coke formation and increase the  
56 carbon conversion. Liu et al. [10] used a two-stage reactor to convert PP into CNTs and  
57 hydrogen-rich gas with HZSM-5 as catalysts, and an optimum temperature (700°C)  
58 was proposed. Wu et al. studied the production of CNTs and syngas study from different  
59 types of plastics with varies of catalysts [11-14].

60 It is known that catalysts play a key role in the growth of CNTs. The catalysts used for  
61 CVD synthesis of CNTs formation normally consist of a transition metal and support.  
62 The transition metal nanoparticles are employed either in oxide or metallic forms.  
63 Nickel, iron, and cobalt are reported as the most effective catalysts due to the high  
64 solubility and high diffusion rate of carbon. For example, Lee et al [15] compared the  
65 performance of Ni, Co and Fe based catalysts for CNTs growth from mixed gases. Fe  
66 was found to be the most active catalyst for CNTs growth under CO/NH<sub>3</sub> gas flow with  
67 a ratio of 18. Apart from these common catalysts, there are also some other types of  
68 metals that have been studied for CNTs formation, such as Cu, Ru, Mn and Cr. Catalysts  
69 for CNTs formation also need an appropriate material as support [16]. Various  
70 substrates have been used for CVD of CNTs synthesis, such as silicon dioxide [14],  
71 alumina [17], quartz, calcium carbonate [18], and zeolite [19]. Fe-Co bimetallic  
72 catalysts supported on CaCO<sub>3</sub> were used as catalysts by Mhlanga et al. [18] to improve  
73 the quality of CNTs with decreasing synthesis time from acetylene. CNTs with outer

74 diameter of 20-30 nm and inner diameter about 10 nm have been successfully produced.

75 Furthermore, many researchers are working on catalyst development to improve the

76 quality of CNTs [13, 20-24].

77 Recently, membrane supported catalysts have emerged, and can be used as a template

78 for CNTs growth to control parameters such as diameter, length, and wall thickness

79 [25]. For example, Golshadi et al. [25] investigated the influence of process parameters

80 (temperature and flow rate) on the CNTs formation (tube wall thickness, CNTs

81 morphology and carbon deposition rate) using anodic aluminum oxidize (AAO)

82 template. It was reported that the yield and wall thickness of the produced CNTs were

83 increased with the increase of reaction temperature to 750 °C; however, further

84 increasing the temperature resulted in a lower production of CNTs. In addition an

85 optimum of gas flow rate was reported for the production of CNTs. Well-aligned CNTs

86 have also been synthesized on glass template from acetylene gas by plasma-enhanced

87 CVD process [26]. Zeolites have also been employed as controlling agents during CNTs

88 growth [27].

89 According to our previous study, AAO membrane catalysts could be used for

90 controlling and improving the quality of CNTs formation [28]. Ceramic membrane

91 (alumina based) was selected as template in this study. This ceramic membrane was

92 provided by AIMR, Aston University, and the properties were studied in Lee's paper

93 [29]. In Lee's paper, ceramic membrane was reported having micro-channel structure,

94 which was similar to our previous research on AAO membrane [28] [29]. This micro-

95 channel structure could control the metal particle loaded inside the membrane and  
96 consequently control the CNTs diameter. However, the yield of CNTs production using  
97 AAO based membrane is low as AAO is difficult to be manufactured in a large scale.  
98 Ceramic membrane has been commercially produced and also has other good properties,  
99 such as high temperature stability, mechanical strength, chemical stability, and low cost  
100 [30, 31]. These properties make ceramic materials one of the best catalytic supports in  
101 the fields of environmental and energy research [31]. Quan et al. produced high quality  
102 syngas from biomass fuel gas over NiO/porous ceramic catalysts [32]. And Gao et al.  
103 studied steam reforming of biomass tar for hydrogen production using NiO/ceramic  
104 foam as catalysts [33]. Membrane catalysts have also shown superior catalytic stability  
105 over equivalent powder [34].

106 The quality of CNTs can significantly affect and limit their applications. For example,  
107 An et al. [35] synthesized CNT composite from the catalytic decomposition of  
108 acetylene over Fe/aluminum ceramic catalyst. It was reported that the CNT content  
109 increased with the increase of Fe content. The mechanical properties of the produced  
110 composite material was also enhanced with the increase of CNTs formation. Flahaut et  
111 al. [36] prepared Fe-Al<sub>2</sub>O<sub>3</sub> ceramics with and without CNTs to study composites  
112 properties, and they found those contained higher quantities of CNTs and much less  
113 nanofibers were good electric conductors. Therefore, experimental conditions (both  
114 reaction temperature and Ni loading) were studied to determine the optimal conditions  
115 for the production of high quality CNTs, which is reflected by a narrow distribution of  
116 CNTs diameter.

117

## 118 **2. Experimental**

### 119 2.1 Materials preparation

120 High density polyethylene plastics (HDPE) pellets with high purity (~ 90%) and a  
121 diameter around 2 mm were provided by Poli Plastic Pellets Ltd. Ceramic membrane  
122 used in this study was made of aluminium oxide, and with 1mm thickness and 30mm  
123 diameter provided by AIMR, Aston University. The original ceramic membrane  
124 preparation and formation method was described in Lee's paper [29]. It is noted that  
125 the BET surface area of the membrane is below 10 m<sup>2</sup>/g. Impurities such as  
126 polyethersulfone was used as binder for membrane preparation. The required amounts  
127 (0.025g for 0.1/ceramic, 0.125g for 0.5/ceramic, 0.251g for 1.0/ceramic, 0.508g for 2.0  
128 ceramic) of Ni (NO<sub>3</sub>)<sub>2</sub>.6H<sub>2</sub>O were dissolved in 5ml ethanol, the mixture liquid was  
129 loaded on each membrane (~1.32g) by dropping the precursors into the membrane. The  
130 obtained wet Ni/ceramic membrane was dried in the oven at 100°C for 24h, then  
131 calcined in air at 800 °C with 10 °C min<sup>-1</sup> heating rate for 3 hours. It is noted that the  
132 Ni/ceramic catalysts prepared from using 0.1, 0.5, 1.0 and 2.0 mol L<sup>-1</sup> Ni (NO<sub>3</sub>)<sub>2</sub>.6H<sub>2</sub>O  
133 was assigned as 0.1/ceramic, 0.5/ceramic, 1.0/ceramic and 2.0/ceramic, respectively in  
134 this paper.

### 135 2.2 CNTs synthesis from catalytic pyrolysis of plastics

136 A two-stage catalytic thermal-chemical conversion reaction system (Fig. 1) consisting  
137 of a plastic pyrolysis stage and a catalytic gasification stage. In each experiment, about

138 1 g HDPE was pyrolysed at around 500 °C at the first stage, Different reaction  
139 temperatures were used in the second stage (600 °C, 700 °C, and 800 °C). N<sub>2</sub> was used  
140 as carrier gas with 100 ml min<sup>-1</sup> flow rate. The total reaction time was 60 mins. The  
141 system was then slowly cooled down to the room temperature with continuous 100 ml  
142 min<sup>-1</sup> N<sub>2</sub> gas. The reacted Ni/ceramic membrane catalyst including the grown CNTs  
143 were collected for further characterizations. The effect of pyrolysis temperature and the  
144 content of Ni on ceramic membrane were studied in relative to their influences on the  
145 growth of CNTs.

### 146 2.3 Sample characterization

147 A scanning electron microscope (SEM) Stereoscan 360 and a high resolution  
148 transmission electron microscope (TEM) JEOL 2010 were used to analyse the surface  
149 and the cross-section morphology of the fresh Ni/ceramic membrane. According to  
150 TEM results, the distribution of diameters of catalyst particles were further analyzed by  
151 Image J software. Sample crystallinity was evaluated by powder X-ray diffraction  
152 (XRD), using Stoe IPDS2 software, with elemental analysis assessed by inductively  
153 coupled plasma mass spectrometry (ICP-MS), ThermoScientific iCAP 7000 ICP  
154 spectrometer after complete sample digestion in conc. Nitric acid. In addition,  
155 temperature program reduction (TPR) was carried out on a Quantachrome Chem BET  
156 3000 system, with samples heated from 50 °C to 700 °C at 10 °C min<sup>-1</sup> under flowing  
157 H<sub>2</sub> (10 ml min<sup>-1</sup>), to observe the catalytic metal reduction.

158 CNTs formation on the Ni/ceramic after reaction was also investigated by SEM and



159 TEM. Distribution of CNTs diameters according to TEM results was carried out using  
160 Image-J software. Temperature programmed oxidation (TPO) of the reacted Ni/ceramic  
161 was analysed to obtain the information of carbon formation on the reacted catalyst.

162

### 163 **3. Results and discussion**

#### 164 3.1 Characterization of fresh Ni/ceramic catalyst

165 Fresh catalysts before reaction with different Ni loadings have been analysed by SEM,  
166 TEM, ICP, XRD and TPR, respectively. SEM results of the surface and the cross section  
167 of the fresh Ni/ceramic catalyst are shown in Fig. 2A and 2B, respectively. The surface  
168 and cross-section show a similar structure; porous structure can be clearly observed  
169 from both pictures. Therefore, SEM images on the surface of materials are used for  
170 following discussion. Based on the XRD results (Fig. 3), the original ceramic  
171 membrane without Ni loading shows diffraction peaks of  $\text{Al}_2\text{O}_3$  [37], indicating the  
172 nature of the ceramic is  $\text{Al}_2\text{O}_3$ . NiO peaks appear at  $63^\circ$  and  $76^\circ$ , respectively, for the  
173 catalyst with different Ni contents loadings [14]. Two  $\text{NiAl}_2\text{O}_4$  peaks appear at around  
174  $37^\circ$  and  $77^\circ$  [38]. ICP results as shown in Table 1 further indicate that the content of  
175 Ni element increased from 0.25 to 3.3 wt. % with the increase of Ni loading. Fig. 4  
176 shows the TEM results (A-D) for the Ni/ceramic samples. The distribution of NiO  
177 diameters was also calculated according to TEM results for the catalyst with different  
178 Ni loadings. Small amount of NiO particles was observed on the surface of the  
179 0.1/ceramic, which has particles with  $11.4 \pm 2.4$  nm diameter, with NiO diameter

180 correlating with metal loading, in agreement with the literature[11], resulting in average  
181 particle size of  $35.2 \pm 3.5$  nm for the 2.0/ceramic (Fig.3 D).

182 TPR results of the fresh Ni/ceramic catalysts are shown in Fig. 5. A major reduction  
183 temperature for all the catalysts occurred between 370 and 450°C, assigned to the  
184 reduction of NiO particles [11]. As shown in Fig. 5, the catalysts were further reduced  
185 at 550 °C which is suggested to the reduction of Ni spinel as observed from the XRD  
186 analysis (Fig.3).

### 187 3.2 Carbon nanotubes production

188 Two reaction parameters using ceramic membrane catalysts with different Ni contents  
189 loading were investigated in relation to the effect on the CNTs formation from plastics  
190 waste. Table 2 is a summary of different reaction parameters (Ni content and reaction  
191 temperature) and CNTs formation analysis (amount of amorphous carbon, filamentous  
192 carbon and CNT average diameter). When the effect of reaction temperature (600, 700,  
193 and 800 °C) was studied, the 0.5/ceramic catalyst was used. When the effect of Ni  
194 content (0.1, 0.5, 1.0 and 2.0) was studied, thermochemical conversion of waste HDPE  
195 was investigated at 700 °C.

196 CNTs formation from thermochemical conversion of plastics waste in this study was  
197 investigated according to both quantitative analysis and qualitative analysis. The  
198 quantitative analysis of CNTs was further discussed based on the yields of amorphous  
199 carbons and filamentous carbons which was obtained by TGA-TPO analysis of the  
200 spent catalysts (Fig. S1 and S2). It is assumed that the oxidation temperature below

201 550 °C was assigned to amorphous carbons and the oxidation above 550 °C in TPO  
202 was assigned to filamentous carbon (assumed as CNTs in this work) [39], two different  
203 types of carbon has been separated and analysed by vertical black imaginary line (Fig.  
204 S1 and S2). The total carbon yield could be represented by X axis ‘the weight loss’ of  
205 catalyst in relation to the initial catalyst weight. The fractions of the two different types  
206 of carbons in relation to the weight of reacted catalysts are summarized in Table 2.

207 In addition, the quality of CNTs production is analysed and discussed mainly based on  
208 the distribution of CNTs diameters and their standard deviations. The average diameter  
209 of CNTs is calculated according to SEM and TEM results using Image J, and  
210 summarized in Table 2 (shown in Fig. S3). The standard deviation (SD) number is used  
211 as a main factor to identify the quality of CNTs formation in this study. In addition, the  
212 ratio of filamentous and amorphous carbon was also discussed in following sections to  
213 obtain the optimum reaction parameter for CNTs formation. A better quality of CNTs  
214 is identified with a smaller SD number and higher ratio of filamentous and amorphous  
215 carbon in this paper.

### 216 3.3 Effect of reaction temperature on CNTs growth

217 The effect of reaction temperature on the growth of CNTs through thermal conversion  
218 from HDPE using Ni/ceramic catalysts is discussed in this section. Three different  
219 reaction temperatures (600°C, 700°C and 800°C) were investigated using the 0.5/  
220 ceramic catalyst. Scanning electron microscope (SEM), transmitted electron  
221 microscope (TEM), temperature program oxidation (TGA-TPO and DTG-TPO)

222 analysis were carried out to the reacted CNTs/catalysts. For SEM results (Fig.6 A-C), a  
223 small amount of uninformed, short filamentous carbons were observed at 600°C (Fig.6A).  
224 CNTs with a diameter around 10 nm and a length around 10 μm is observed at catalytic  
225 reaction temperature of 600 °C. This result is similar to literature where Ni/Al<sub>2</sub>O<sub>3</sub> was  
226 used for producing CNTs from waste plastics [14].

227 With the increase of reaction temperature to 700°C (Fig.6B), a large amount of  
228 filamentous carbons with long length are found on the ceramic membrane. However,  
229 when the reaction temperature was further increased to 800°C, only a few filamentous  
230 carbons could be observed on the surface of the catalyst (Fig.6C). The SEM results of  
231 the reacted catalyst were further supported by TEM analysis (Fig. 6 i-iii). CNTs with  
232 diameter  $21.2 \pm 5.6$  and  $16.9 \pm 4.3$  nm were clearly observed in Fig. 6 i and ii,  
233 respectively. It is difficult to find CNTs on the catalyst reacted at 800 °C (Fig.6 iii).  
234 Therefore, it is suggested that 700 °C is an optimal reaction temperature for the  
235 formation of CNTs from waste plastics in this work. Similar results were reported by  
236 Li et al [40], who studied various temperatures from 600°C to 1050°C for CNTs  
237 production from C<sub>2</sub>H<sub>2</sub> with Fe/SiO<sub>2</sub> catalysts. They reported minimal CNTs yield at  
238 either low (600°C) or high (1050°C) temperature.

239 This result is further supported by carbon production analysis (Table 2). For amorphous  
240 carbons (oxidation temperature below 550 °C), the yield was decreased from 2.1 to 1.2  
241 wt. %, when the temperature increased from 600 °C to 700 °C. This result is consistent  
242 with the SEM analysis (Fig. 6), where amorphous carbons could be clearly observed on

243 the reacted catalyst tested at 600 °C. Furthermore, the formation of CNTs was reduced  
244 from 7.2 wt. % and 1.2 wt. % when the reaction temperature was increased 600°C and  
245 800°C. DTG-TPO results (Fig.7) with DCS (Differential Scanning Calorimetry)  
246 showed that the oxidation peak moved to higher temperature with the increase of  
247 experimental temperature from 600°C and 700°C, indicating that the CNTs might be  
248 more crystalized at 700°C reaction temperature. Similar results were also reported by  
249 Hornyak et al. [41], who investigated the template synthesis of CNTs formation on  
250 porous alumina membrane (PAM) from propylene gas with Co-based catalysts. They  
251 reported that amorphous carbon was formed at around 550°C, while CNTs was formed  
252 at temperature higher than 800°C. The starting temperature for CVD synthesis of CNTs  
253 was normally over 500°C [42-44].

254 It is suggested that the effect of reaction temperature on CNTs synthesis by CVD was  
255 mainly related to carbon source and catalytic sites. CNTs growth can be described as  
256 following steps, first carbon atoms from the dissociation of hydrocarbons dissolve into  
257 the catalytic metal sites. The diffused carbon atoms form graphitic sheets on the surface  
258 of metal particles [45]. The diffusion of carbon atoms is a main factor to determine the  
259 CNTs formation. The increasing temperature can promote the diffusion rate of carbon  
260 atoms, as a result, CNTs are synthesised with less defect. Lee et al. [46] and Mishra et  
261 al. [47] also reported that an increase of temperature promoted the diffusion and  
262 reaction rates of carbons, resulting in the enhanced formation of CNTs. In addition, Wu  
263 and Williams [48] reported that at high temperature, more reactive carbon sources were  
264 produced from pyrolysis of waste plastics. Therefore, in this study, less amorphous

265 carbons were form at 700°C compared to 600°C, which supported by SEM and TPO  
266 analysis. Similar results were reported by Acomb et al. [49] who carried out the effect  
267 of growth temperature (700 °C, 800 °C, and 900 °C) on the CNTs production using low  
268 density polyethylene (LDPE) with Fe/Al<sub>2</sub>O<sub>3</sub> as catalyst. They found that a lower  
269 temperature produced less fraction of CNTs.

270 However, when the reaction temperature is too high, the sintering of catalytic sites  
271 could occur, which is responsible for the deactivation of catalysts [43]. Also, the excess  
272 of carbon atoms accumulated on the surface of catalyst could encapsulate catalytic sites  
273 causing catalyst deactivation. For example, Hanaei et al. [50] investigated the influence  
274 of reaction temperatures (550°C-950°C) on CNTs from acetone with Fe-Mo/Al<sub>2</sub>O<sub>3</sub>  
275 catalysts. 750°C was reported as an ideal temperature as the deactivation of catalysts  
276 occurred at higher temperature. Toussi et al. [51] reported the similar conclusion on  
277 CNTs synthesis from ethanol deposited on Fe-Mo-MgO catalyst; when temperature was  
278 lower than 750°C, few CNTs could be produced. And the optimum growth of CNTs  
279 was reported at 850°C. Kukoitsky et al. [52] reported an optimal temperature of 700°C  
280 for the growth of CNTs from polyethylene with Ni-based catalyst at 700°C; as narrow  
281 size distribution of CNTs was found at 700°C than those grown at 800°C, due to the  
282 loss of catalytic activity for CNTs forming at high temperature. In this study, it is  
283 noticed that there was little CNTs formed at 800°C (Fig. 6 and 7), which we attribute to  
284 loss of catalytic active sites at high temperature due to sintering As shown in Fig. 6iii,  
285 almost no CNTs production could be observed from TEM results. The diameter of NiO  
286 particles before reaction was 17.9±4.4 nm (Fig. 4B), however, large amount of large

287 catalytic particles with diameter 52-78 nm could be observed after reaction (Fig. 6iii).  
288 Overall, Fig. 8 summarizes the trends of SD of CNTs diameter and ratio of filamentous  
289 amorphous carbon as increasing reaction temperature. CNTs show the smallest SD and  
290 highest filamentous / amorphous carbon ratio at 700 °C reaction temperature. Therefore,  
291 700°C was assumed as the optimum temperature for this study.

### 292 3.4 Effect of Ni content on the production of CNTs

293 In this section, thermochemical conversion of waste HDPE was investigated in the  
294 presence of Ni/ceramic catalysts with different Ni contents at 700°C. Fig.8 showed the  
295 SEM results and corresponding TEM results for the filamentous carbon production  
296 using the Ni/ceramic catalysts. With the increase of Ni loading, more filamentous  
297 carbons could be observed from SEM results. In particular, for the reacted 0.1/ceramic  
298 catalyst, the formation of filamentous carbons can be barely found. It is indicated that  
299 the 0.1/ceramic and 0.5/ceramic catalysts might have small amount of active metals  
300 loaded on the ceramic membrane. TEM results (Fig.8 i-v) further proved that the  
301 filaments carbons are mostly CNTs. The average diameter of CNTs (Table 2) was  
302 analysed according to the TEM results. It could be noticed that the diameter of CNTs  
303 increased with an increase of Ni content. The 0.1/ceramic had the smallest diameter  
304  $15.7\pm 3.6$  nm, and the 2.0/ceramic had the largest diameter  $24.9\pm 2.3$  nm, in close  
305 agreement with the average sizes of the NiO nanoparticles. The changes of diameters  
306 of CNTs showed a similar trend with the metal particles size as shown in Fig. 10, where  
307 the particle size of NiO was increased with the increase of metal loading. Similar results

308 were also found by other researchers [53]. Sinnott et al. [53] studied the effect of Fe  
309 content on the diameter of CNTs produced from ferrocene-xylene mixture through  
310 chemical vapour deposition. They reported that the average Fe particle size was  
311 decreased from 35.3 to 28.2 nm with a decrease of Fe content from 0.75 to 0.075 at%  
312 and the lower Fe content resulted in the production of less CNTs. Li et al. [54]  
313 synthesised CNTs from methane and hydrogen mixture using Fe<sub>2</sub>O<sub>3</sub>-based catalysts  
314 with a range of 1-2nm and 3-5 nm respectively. CNTs with diameters of 1.5±0.4 nm  
315 and 3.0±0.9 nm were produced, respectively. The CNTs could be diffused by catalytic  
316 metal particles during growth process, therefore, the size of metal particles determine  
317 the diameter of filamentous carbons [53]. For example, Cheung et al. [55] used iron  
318 nanoparticles with average diameters of 3, 9, and 13nm to grow CNTs with average  
319 diameters of 3, 7, and 12 nm from ethylene, respectively.

320 The size of metal particles have also been reported to affect the activity of catalysts and  
321 the formation of CNTs [55-60]. In addition, loading various amounts of metal on  
322 catalyst normally results in the formation of catalyst with various metal particle sizes,  
323 as obtain in this work, to control the production of CNTs. Daudouin et al. increased the  
324 Ni loading from 1.0 wt.% to 18.5 wt.% to increase the catalytic particle sizes from 1.6  
325 to 7.3 nm [61]. The diameter of metal particles was increased with the increase of metal  
326 loading. In addition, CNTs with larger diameters were produced with the increase of  
327 metal loading. However, a maximum diameter of CNTs should be expected, when the  
328 loading of metal in the catalyst is too high. For example, Chen et al. [62] referred to an  
329 optimally size of catalyst which could produce an optimum growth rate and a high yield



330 of carbon nanofibers (CNFs). They reported that smaller ( $< 20\text{nm}$ ) Ni crystals caused a  
331 slow growth of CNFs and a fast deactivation of catalyst. However, when the metal  
332 particles were larger than  $60\text{nm}$ , the rate of CNFs growth was prohibited due to the low  
333 surface area of active sites. Danafar et al.[57] studied Fe-Co/Al catalysts with 6 ranges  
334 of metal particle sizes to study the influence on the synthesis of CNTs from ethanol.  
335 They found that the catalyst with  $10\text{-}20\ \mu\text{m}$  metal particles produced about 30% higher  
336 carbon yield than the catalyst having the largest catalytic particles. It is reported that  
337 the catalysts with smaller diameters had larger breaking through capacities during  
338 frontal diffusion (shorter diffusion path length). In addition, the catalyst with large  
339 metal particle size produced more amorphous carbons and uninform CNTs, as the  
340 stability of metal agglomerates decreased with increasing particle sizes.

341 According to Table 2 and DTG-TPO (Fig. 11) analysis of the reacted catalysts with  
342 different Ni loadings, a maximum production of CNTs was obtained in the presence of  
343 the 1.0/ceramic catalyst. CNTs production was increased from 3.1 to 9.4 wt %, when  
344 the catalyst was changed from the 0.1/ceramic to the 1.0/ceramic. Similar results have  
345 been discussed by other researchers. For example, Venegoni et al. [63] studied the effect  
346 of Fe content (0.5%, 1%, 2% and 5%) on CNTs growth in the presence of Fe/SiO<sub>2</sub>  
347 catalysts from a mixture of H<sub>2</sub> and C<sub>2</sub>H<sub>4</sub>. Catalyst with the most amount of Fe metal  
348 content (5% Fe-SiO<sub>2</sub>) was least active in relation to the production of CNTs, due to the  
349 presence of large metal particles. In addition, it was reported that the active catalytic  
350 sites was increased to promote catalytic reactions with increasing catalytic metal  
351 content until an optimal value was reached [64]. In this study, the

352 filamentous/amorphous carbon ratio was the highest about 5 with the 0.5/ceramic  
353 catalyst used (Fig. 12), then slightly decreased to about 4.7 when the catalyst was  
354 changed to the 1.0/ceramic. However, the 0.5/ceramic catalyst showed the highest SD  
355 number (Fig. 12). Overall, considering the filamentous/amorphous carbon ratio and SD  
356 of CNTs diameter, the 1.0/ceramic catalyst was suggested to be a better candidate for  
357 CNTs formation from thermochemical conversion from plastic waste.

358

#### 359 **4. Conclusions**

360 Carbon nanotubes formation from catalytic thermo-chemical conversion of waste  
361 plastics using ceramic membrane based catalyst was optimized in this work in relation  
362 to metal loading and reaction temperature. An optimum temperature 700° was  
363 suggested for Ni-based ceramics membrane. An increase of Ni content on ceramic  
364 membrane resulted in increasing diameters of metal particle sizes which could affect  
365 the activity of catalysts and the formation of CNTs. The 1.0/ceramic was the optimum  
366 candidate for CNTs formation in this study giving the highest fraction of filamentous  
367 carbons with the narrowest distribution of CNTs diameter.

368

#### 369 **Acknowledgement**

370 The authors would like to thank The University of Hull, UK and Hebei University of  
371 Technology, China for the financial support towards this research work.

372

373 **References**

- 374 [1] WRAP. Plastics Market Situation Report. (Spring 2016).
- 375 [2] S.M. Al-Salem, P. Lettieri, J. Baeyens. Recycling and recovery routes of plastic  
376 solid waste (PSW): A review. *Waste Management*. 29 (2009) 2625-43.
- 377 [3] A. Erkiaga, G. Lopez, I. Barbarias, M. Artetxe, M. Amutio, J. Bilbao, et al. HDPE  
378 pyrolysis-steam reforming in a tandem spouted bed-fixed bed reactor for H<sub>2</sub> production.  
379 *Journal of Analytical and Applied Pyrolysis*. 116 (2015) 34-41.
- 380 [4] B.B. Gershman, Inc. Gasification of Non-Recycled Plastics From Municipal Solid  
381 Waste In the United States. solid waste management consultants. GBB/12038 (2013).
- 382 [5] V.M.O.L. L.V. Radushkevich. Structure uglieroda, obrazujucesja pri termiceskom  
383 razlozenii okisi uglieroda na zeleznom kontakte. *Zurn Fisic Chim*. 26 (1952) 88-95.
- 384 [6] S. Iijima. Helical microtubules of graphitic carbon. *Nature*. 354 (1991) 56-8.
- 385 [7] Cheaptubes. Industrial carbon nanotubes products. 2018.
- 386 [8] M. Trojanowicz. Analytical applications of carbon nanotubes: a review. *TrAC*  
387 *Trends in Analytical Chemistry*. 25 (2006) 480-9.
- 388 [9] Y. Park, T. Namioka, S. Sakamoto, T.-j. Min, S.-a. Roh, K. Yoshikawa. Optimum  
389 operating conditions for a two-stage gasification process fueled by polypropylene by  
390 means of continuous reactor over ruthenium catalyst. *Fuel Processing Technology*. 91  
391 (2010) 951-7.
- 392 [10] J. Liu, Z. Jiang, H. Yu, T. Tang. Catalytic pyrolysis of polypropylene to synthesize  
393 carbon nanotubes and hydrogen through a two-stage process. *Polymer Degradation and*  
394 *Stability*. 96 (2011) 1711-9.
- 395 [11] C. Wu, L. Wang, P.T. Williams, J. Shi, J. Huang. Hydrogen production from  
396 biomass gasification with Ni/MCM-41 catalysts: Influence of Ni content. *Applied*  
397 *Catalysis B: Environmental*. 108–109 (2011) 6-13.
- 398 [12] C. Wu, P.T. Williams. Hydrogen Production from the Pyrolysis–Gasification of  
399 Polypropylene: Influence of Steam Flow Rate, Carrier Gas Flow Rate and Gasification  
400 Temperature. *Energy & Fuels*. 23 (2009) 5055-61.
- 401 [13] J.C. Acomb, C. Wu, P.T. Williams. The use of different metal catalysts for the  
402 simultaneous production of carbon nanotubes and hydrogen from pyrolysis of plastic  
403 feedstocks. *Applied Catalysis B: Environmental*. 180 (2016) 497-510.
- 404 [14] X. Liu, Y. Zhang, M.A. Nahil, P.T. Williams, C. Wu. Development of Ni- and Fe-

405 based catalysts with different metal particle sizes for the production of carbon  
406 nanotubes and hydrogen from thermo-chemical conversion of waste plastics. *Journal*  
407 *of Analytical and Applied Pyrolysis*.

408 [15] T.Y. Lee, J.-H. Han, S.H. Choi, J.-B. Yoo, C.-Y. Park, T. Jung, et al. Comparison  
409 of source gases and catalyst metals for growth of carbon nanotube. *Surface and*  
410 *Coatings Technology*. 169–170 (2003) 348-52.

411 [16] K.A. Shah, B.A. Tali. Synthesis of carbon nanotubes by catalytic chemical vapour  
412 deposition: A review on carbon sources, catalysts and substrates. *Materials Science in*  
413 *Semiconductor Processing*. 41 (2016) 67-82.

414 [17] Y.C. Sui, B.Z. Cui, R. Guardián, D.R. Acosta, L. Martínez, R. Perez. Growth of  
415 carbon nanotubes and nanofibres in porous anodic alumina film. *Carbon*. 40 (2002)  
416 1011-6.

417 [18] S.D. Mhlanga, K.C. Mondal, R. Carter, M.J. Witcomb, N.J. Coville. The effect of  
418 synthesis parameters on the catalytic synthesis of multiwalled carbon nanotubes using  
419 Fe-Co/CaCO<sub>3</sub> catalysts. *South African Journal of Chemistry*. 62 (2009) 67-76.

420 [19] M. Kumar, Y. Ando. Controlling the diameter distribution of carbon nanotubes  
421 grown from camphor on a zeolite support. *Carbon*. 43 (2005) 533-40.

422 [20] H. Ago, N. Uehara, N. Yoshihara, M. Tsuji, M. Yumura, N. Tomonaga, et al. Gas  
423 analysis of the CVD process for high yield growth of carbon nanotubes over metal-  
424 supported catalysts. *Carbon*. 44 (2006) 2912-8.

425 [21] G. Bajad, V. Guguloth, R.P. Vijayakumar, S. Bose. Conversion of plastic waste  
426 into CNTs using Ni/Mo/MgO catalyst An optimization approach by mixture experiment.  
427 *Fullerenes Nanotubes and Carbon Nanostructures*. 24 (2016) 162-9.

428 [22] N. Borsodi, A. Szentes, N. Miskolczi, C. Wu, X. Liu. Carbon nanotubes  
429 synthesized from gaseous products of waste polymer pyrolysis and their application.  
430 *Journal of Analytical and Applied Pyrolysis*. 120 (2016) 304-13.

431 [23] G. Che, B.B. Lakshmi, C.R. Martin, E.R. Fisher, R.S. Ruoff. Chemical Vapor  
432 Deposition Based Synthesis of Carbon Nanotubes and Nanofibers Using a Template  
433 Method. *Chemistry of Materials*. 10 (1998) 260-7.

434 [24] H.M. Cheng, F. Li, G. Su, H.Y. Pan, L.L. He, X. Sun, et al. Large-scale and low-  
435 cost synthesis of single-walled carbon nanotubes by the catalytic pyrolysis of  
436 hydrocarbons. *Applied Physics Letters*. 72 (1998) 3282-4.

437 [25] M. Golshadi, J. Maita, D. Lanza, M. Zeiger, V. Presser, M.G. Schrlau. Effects of

438 synthesis parameters on carbon nanotubes manufactured by template-based chemical  
439 vapor deposition. *Carbon*. 80 (2014) 28-39.

440 [26] Z.F. Ren, Z.P. Huang, J.W. Xu, J.H. Wang, P. Bush, M.P. Siegal, et al. Synthesis of  
441 large arrays of well-aligned carbon nanotubes on glass. *Science* (New York, NY). 282  
442 (1998) 1105-7.

443 [27] W. Zhao, B. Basnet, I.J. Kim. Carbon nanotube formation using zeolite template  
444 and applications. *Journal of Advanced Ceramics*. 1 (2012) 179-93.

445 [28] X. Liu, H. Sun, C. Wu, D. Patel, J. Huang. Thermal Chemical Conversion of High-  
446 Density Polyethylene for the Production of Valuable Carbon Nanotubes Using Ni/AAO  
447 Membrane Catalyst 2017.

448 [29] M. Lee, B. Wang, Z. Wu, K. Li. Formation of micro-channels in ceramic  
449 membranes – Spatial structure, simulation, and potential use in water treatment. *Journal*  
450 *of Membrane Science*. 483 (2015) 1-14.

451 [30] E.T. Thostenson, Z. Ren, T.-W. Chou. Advances in the science and technology of  
452 carbon nanotubes and their composites: a review. *Composites Science and Technology*.  
453 61 (2001) 1899-912.

454 [31] N. Labhsetwar, P. Doggali, S. Rayalu, R. Yadav, T. Mistuhashi, H. Haneda.  
455 *Ceramics in Environmental Catalysis: Applications and Possibilities*. *Chinese Journal*  
456 *of Catalysis*. 33 (2012) 1611-21.

457 [32] C. Quan, N. Gao, C. Wu. Utilization of NiO/porous ceramic monolithic catalyst  
458 for upgrading biomass fuel gas. *Journal of the Energy Institute*.

459 [33] N. Gao, S. Liu, Y. Han, C. Xing, A. Li. Steam reforming of biomass tar for  
460 hydrogen production over NiO/ceramic foam catalyst. *International Journal of*  
461 *Hydrogen Energy*. 40 (2015) 7983-90.

462 [34] Y. Liu, M. Peng, H. Jiang, W. Xing, Y. Wang, R. Chen. Fabrication of ceramic  
463 membrane supported palladium catalyst and its catalytic performance in liquid-phase  
464 hydrogenation reaction. *Chemical Engineering Journal*. 313 (2017) 1556-66.

465 [35] J.W. An, D.H. You, D.S. Lim. Tribological properties of hot-pressed alumina–CNT  
466 composites. *Wear*. 255 (2003) 677-81.

467 [36] E. Flahaut, A. Peigney, C. Laurent, C. Marlière, F. Chastel, A. Rousset. Carbon  
468 nanotube–metal–oxide nanocomposites: microstructure, electrical conductivity and  
469 mechanical properties. *Acta Materialia*. 48 (2000) 3803-12.

470 [37] V. Muñoz, A.G.T. Martinez. Thermal Evolution of Al<sub>2</sub>O<sub>3</sub>-MgO-C Refractories.

471 Procedia Materials Science. 1 (2012) 410-7.

472 [38] J. Zygmuntowicz, P. Wiecińska, A. Miazga, K. Konopka. Characterization of  
473 composites containing NiAl<sub>2</sub>O<sub>4</sub> spinel phase from Al<sub>2</sub>O<sub>3</sub>/NiO and Al<sub>2</sub>O<sub>3</sub>/Ni systems.  
474 Journal of Thermal Analysis and Calorimetry. 125 (2016) 1079-86.

475 [39] C. Wu, M.A. Nahil, M. Norbert, J. Huang, P.T. Williams. Production and  
476 application of carbon nanotubes, as a co-product of hydrogen from the pyrolysis-  
477 catalytic reforming of waste plastic. Process Safety and Environmental Protection.

478 [40] W.Z. Li, J.G. Wen, Z.F. Ren. Effect of temperature on growth and structure of  
479 carbon nanotubes by chemical vapor deposition. Applied Physics A. 74 (2002) 397-402.

480 [41] G.L. Hornyak, A.C. Dillon, P.A. Parilla, J.J. Schneider, N. Czap, K.M. Jones, et al.  
481 Template synthesis of carbon nanotubes. Nanostructured Materials. 12 (1999) 83-8.

482 [42] A. Aqel, K.M.M.A. El-Nour, R.A.A. Ammar, A. Al-Warthan. Carbon nanotubes,  
483 science and technology part (I) structure, synthesis and characterisation. Arabian  
484 Journal of Chemistry. 5 (2012) 1-23.

485 [43] F. Danafar, A. Fakhru'l-Razi, M.A.M. Salleh, D.R.A. Biak. Fluidized bed catalytic  
486 chemical vapor deposition synthesis of carbon nanotubes—A review. Chemical  
487 Engineering Journal. 155 (2009) 37-48.

488 [44] B.R. Stoner, B. Brown, J.T. Glass. Selected Topics on the Synthesis, Properties  
489 and Applications of Multiwalled Carbon Nanotubes. Diamond and related materials. 42  
490 (2014) 49-57.

491 [45] K.-E. Kim, K.-J. Kim, W.S. Jung, S.Y. Bae, J. Park, J. Choi, et al. Investigation on  
492 the temperature-dependent growth rate of carbon nanotubes using chemical vapor  
493 deposition of ferrocene and acetylene. Chemical Physics Letters. 401 (2005) 459-64.

494 [46] C.J. Lee, J. Park, Y. Huh, J. Yong Lee. Temperature effect on the growth of carbon  
495 nanotubes using thermal chemical vapor deposition. Chemical Physics Letters. 343  
496 (2001) 33-8.

497 [47] N. Mishra, G. Das, A. Ansaldo, A. Genovese, M. Malerba, M. Povia, et al.  
498 Pyrolysis of waste polypropylene for the synthesis of carbon nanotubes. Journal of  
499 Analytical and Applied Pyrolysis. 94 (2012) 91-8.

500 [48] C. Wu, P.T. Williams. Pyrolysis–gasification of post-consumer municipal solid  
501 plastic waste for hydrogen production. International Journal of Hydrogen Energy. 35  
502 (2010) 949-57.

503 [49] J.C. Acomb, C. Wu, P.T. Williams. Effect of growth temperature and

504 feedstock:catalyst ratio on the production of carbon nanotubes and hydrogen from the  
505 pyrolysis of waste plastics. *Journal of Analytical and Applied Pyrolysis*. 113 (2015)  
506 231-8.

507 [50] A.F.I.-R. Hengameh Hanaei<sup>1, 2,\*</sup>, Dayang Radiah Awang Biak<sup>2</sup>, Intan Salwani  
508 Ahamad<sup>2</sup> and Firoozeh Danafar. Effects of Synthesis Reaction Temperature,  
509 Deposition Time and Catalyst on Yield of Carbon Nanotubes. *Asian Journal of*  
510 *Chemistry*. 24 (2010) 2407-14.

511 [51] T. Setareh Monshi, A. Fakhru'l-Razi, A. Luqman Chuah, A.R. Suraya.  
512 Optimization of Synthesis Condition for Carbon Nanotubes by Catalytic Chemical  
513 Vapor Deposition (CCVD). *IOP Conference Series: Materials Science and Engineering*.  
514 17 (2011) 012003.

515 [52] E.F. Kukovitsky, S.G. L'Vov, N.A. Sainov, V.A. Shustov, L.A. Chernozatonskii.  
516 Correlation between metal catalyst particle size and carbon nanotube growth. *Chemical*  
517 *Physics Letters*. 355 (2002) 497-503.

518 [53] S.B. Sinnott, R. Andrews, D. Qian, A.M. Rao, Z. Mao, E.C. Dickey, et al. Model  
519 of carbon nanotube growth through chemical vapor deposition. *Chemical Physics*  
520 *Letters*. 315 (1999) 25-30.

521 [54] Y. Li, W. Kim, Y. Zhang, M. Rolandi, D. Wang, H. Dai. Growth of Single-Walled  
522 Carbon Nanotubes from Discrete Catalytic Nanoparticles of Various Sizes. *The Journal*  
523 *of Physical Chemistry B*. 105 (2001) 11424-31.

524 [55] C.L. Cheung, A. Kurtz, H. Park, C.M. Lieber. Diameter-Controlled Synthesis of  
525 Carbon Nanotubes. *The Journal of Physical Chemistry B*. 106 (2002) 2429-33.

526 [56] A.L.M. da Silva, J.P. den Breejen, L.V. Mattos, J.H. Bitter, K.P. de Jong, F.B.  
527 Noronha. Cobalt particle size effects on catalytic performance for ethanol steam  
528 reforming – Smaller is better. *Journal of Catalysis*. 318 (2014) 67-74.

529 [57] F. Danafar, A. Fakhru'l-Razi, M.A. Mohd Salleh, D.R. Awang Biak. Influence of  
530 catalytic particle size on the performance of fluidized-bed chemical vapor deposition  
531 synthesis of carbon nanotubes. *Chemical Engineering Research and Design*. 89 (2011)  
532 214-23.

533 [58] A. Gorbunov, O. Jost, W. Pompe, A. Graff. Role of the catalyst particle size in the  
534 synthesis of single-wall carbon nanotubes. *Applied Surface Science*. 197–198 (2002)  
535 563-7.

536 [59] C. Lastoskie, K.E. Gubbins, N. Quirke. Pore size distribution analysis of

537 microporous carbons: a density functional theory approach. *The Journal of Physical*  
538 *Chemistry*. 97 (1993) 4786-96.

539 [60] R.J.W. R.T.K. Baker. Formation of carbonaceous deposits from the platinum-iron  
540 catalyzed decomposition of acetylene. *Journal of Catalysis*. 37 (1975) 101-5.

541 [61] D. Baudouin, U. Rodemerck, F. Krumeich, A.d. Mallmann, K.C. Szeto, H. Ménard,  
542 et al. Particle size effect in the low temperature reforming of methane by carbon dioxide  
543 on silica-supported Ni nanoparticles. *Journal of Catalysis*. 297 (2013) 27-34.

544 [62] D. Chen, K.O. Christensen, E. Ochoa-Fernández, Z. Yu, B. Tøtdal, N. Latorre, et  
545 al. Synthesis of carbon nanofibers: effects of Ni crystal size during methane  
546 decomposition. *Journal of Catalysis*. 229 (2005) 82-96.

547 [63] D. Venegoni, P. Serp, R. Feurer, Y. Kihn, C. Vahlas, P. Kalck. Parametric study for  
548 the growth of carbon nanotubes by catalytic chemical vapor deposition in a fluidized  
549 bed reactor. *Carbon*. 40 (2002) 1799-807.

550 [64] F. Melo, N. Morlanés. Naphtha steam reforming for hydrogen production.  
551 *Catalysis Today*. 107–108 (2005) 458-66.

552

553

554

555



556

557

<b>Table 1 - ICP results of Ni/ceramic catalysts with different Ni contents</b>				
<b>catalysts</b>	<b>0.1 / ceramic</b>	<b>0.5 / ceramic</b>	<b>1.0 / ceramic</b>	<b>2.0 / ceramic</b>
<b>Ni content wt.%</b>	<b>0.25</b>	<b>1.1</b>	<b>2.1</b>	<b>3.3</b>

558

559

560

561

562

563

564

565

566

567

568

569

570

571

572

573

574

575

576

577

578

579

580

581

**Table 2 – Overall view of experiments parameters and carbon depositions**

	Ni Content ( <i>molL</i> <sup>-1</sup> )	Temperature (°C)	Amorphous Carbon (%)	Filamentous Carbon (%)	CNTs Average Diameter ( <i>nm</i> )
Effect of the Ni content	0.1	700	1.1	3.1	15.7 ± 3.6
	0.5	700	1.2	6.0	16.9 ± 4.3
	1.0	700	2.0	9.4	20.8 ± 1.9
	2.0	700	2.2	8.0	24.9 ± 2.3
Effect of temperature	0.5	600	2.1	7.2	21.2 ± 5.6
	0.5	700	1.2	6.0	16.9 ± 4.3
	0.5	800	1.2	1.2	-

582

583

584

585

586

587

588

589

590

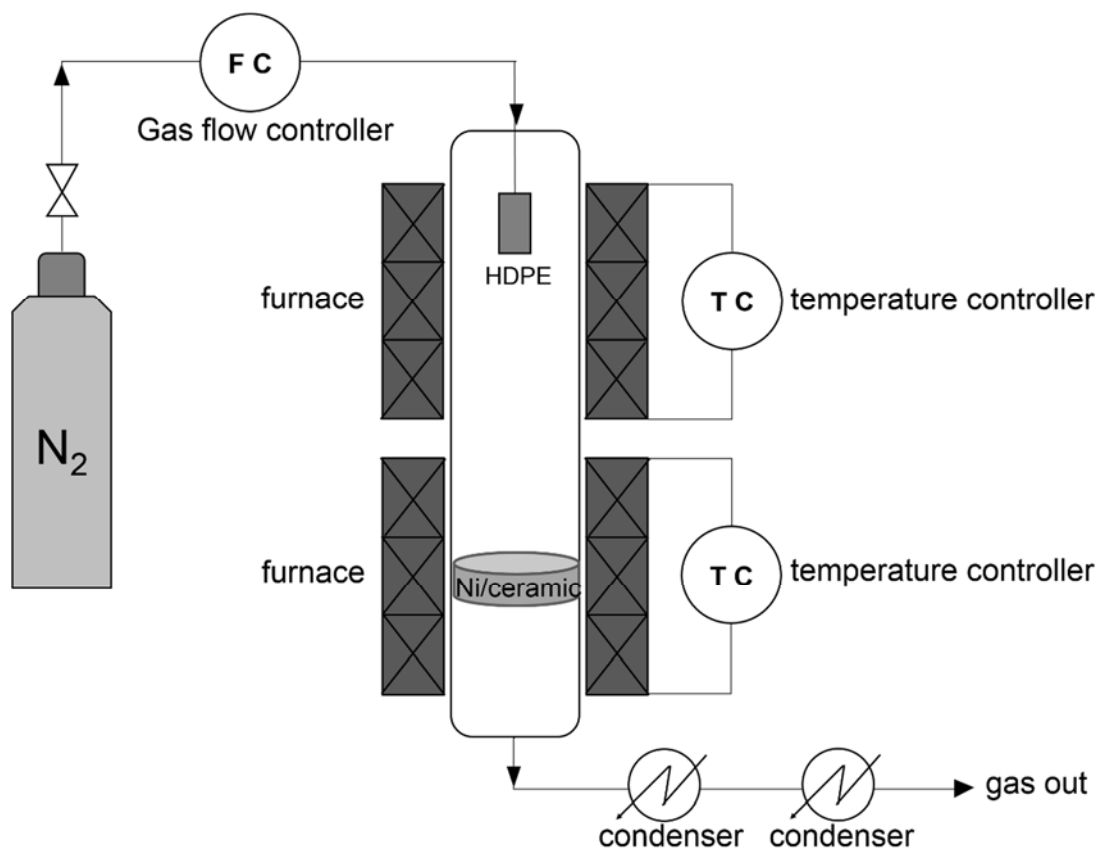
591

592

593

594

595



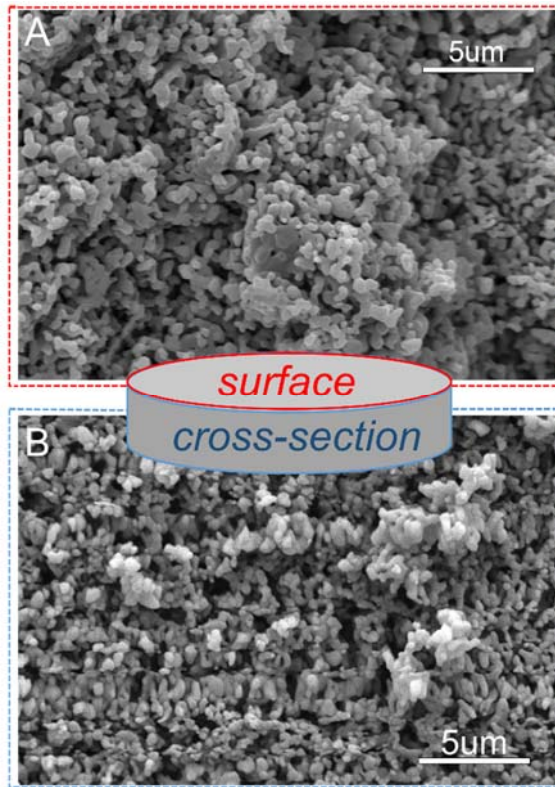
596

597 Fig. 1 A schematic diagram of the reactor for the synthesis CNTs from waste plastics

598

599

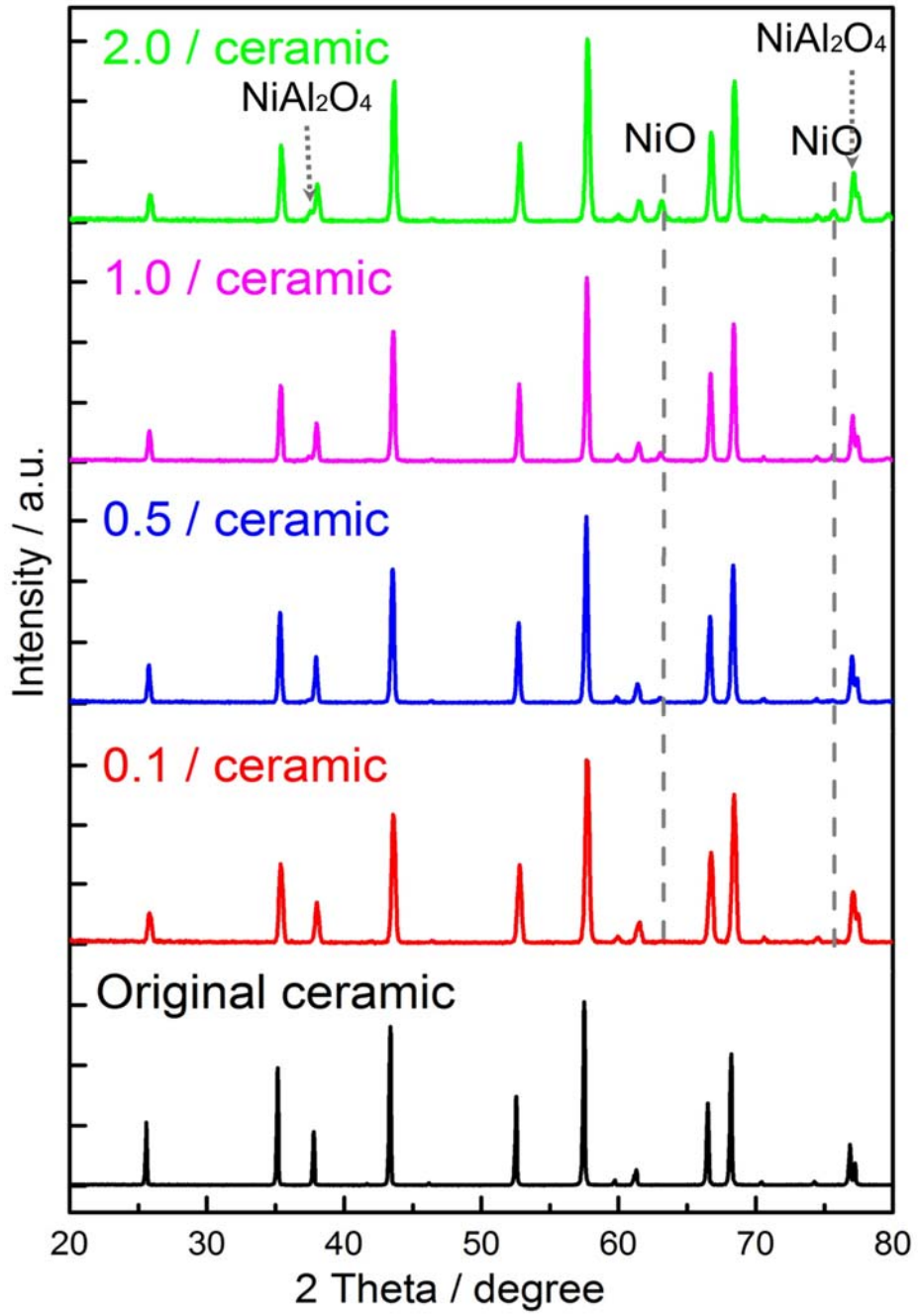
600



601

602 Fig. 2 SEM results for original ceramic membrane (A) surface, (B) cross-section

603



604

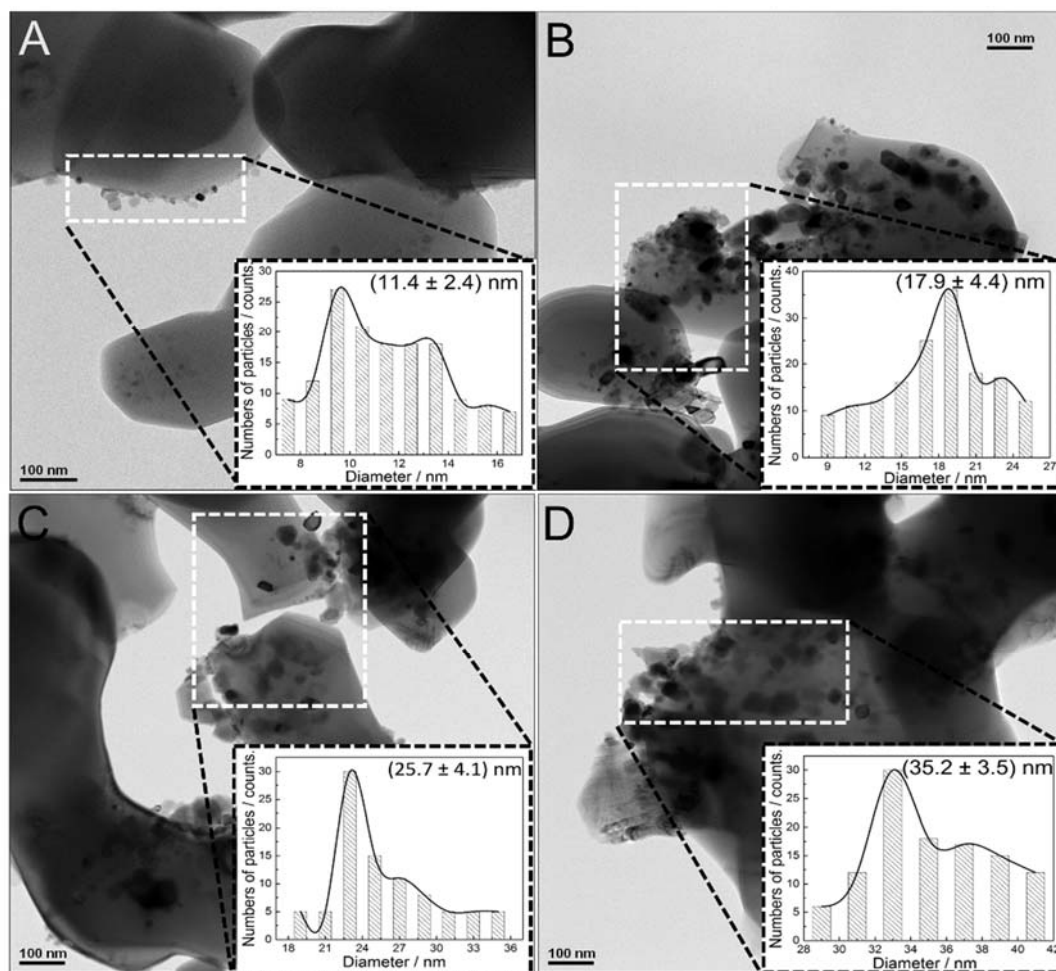
605 Fig. 3 XRD analysis for original ceramic membrane and fresh Ni/ceramic catalysts

606

607

608

609



611

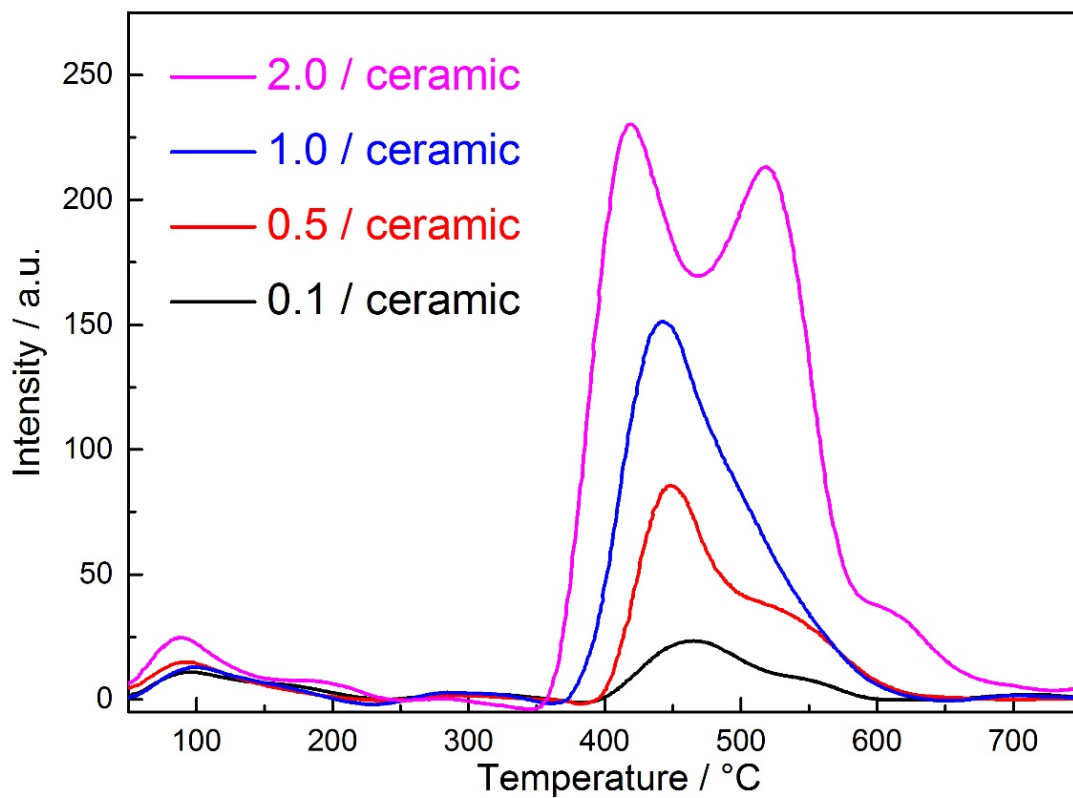
612 Fig. 4 TEM results and diameter distribution of NiO for (A) 0.1, (B) 0.5, (C) 1.0 and

613

(D) 2.0 fresh Ni/ceramic catalysts

614

615



616

617 Fig. 5 TPR analysis of the Ni/ceramic catalysts with different Ni content loadings

618

(0.1, 0.5, 1.0, and 2.0 Ni mol/L)

619

620

621

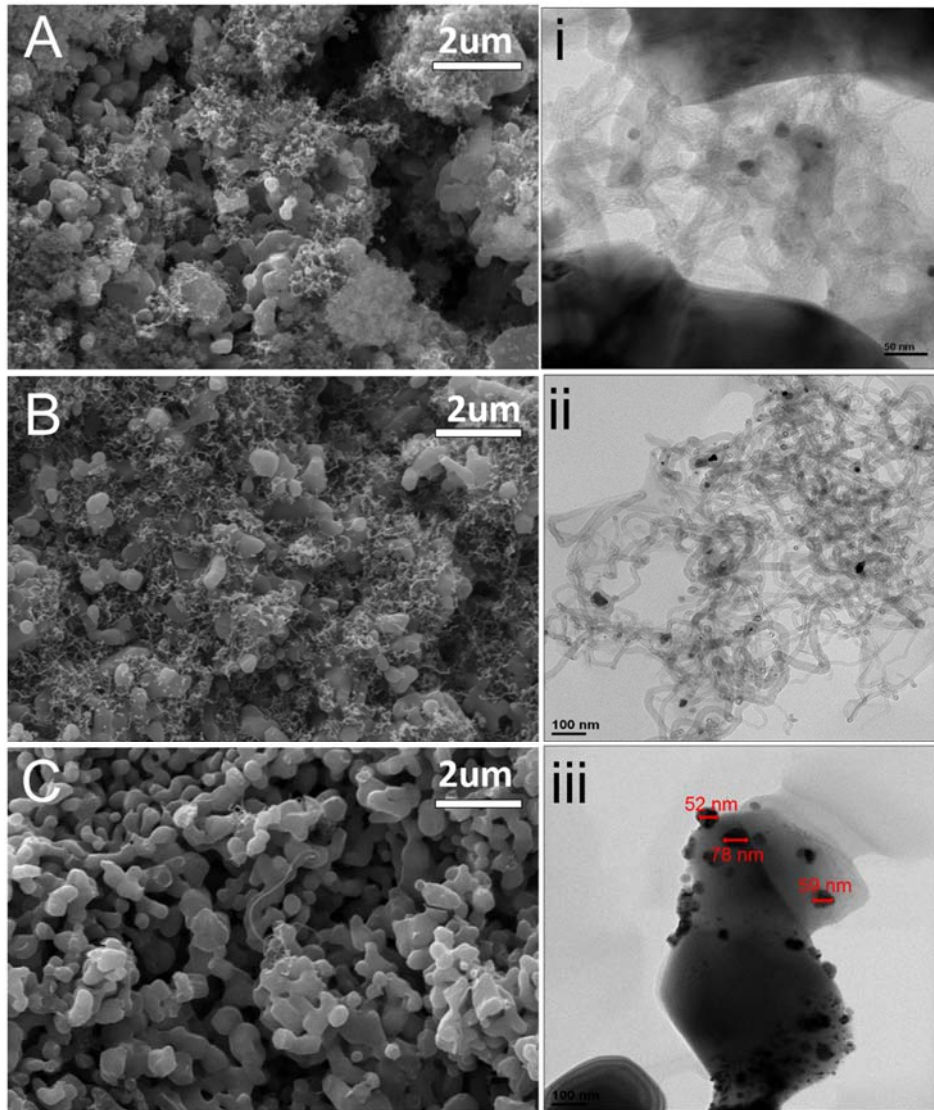
622

623

624

625

626



627

628 Fig. 6 SEM (left) and TEM (right) results for CNTs synthesis at (A) 600°C, (B) 700°C

629

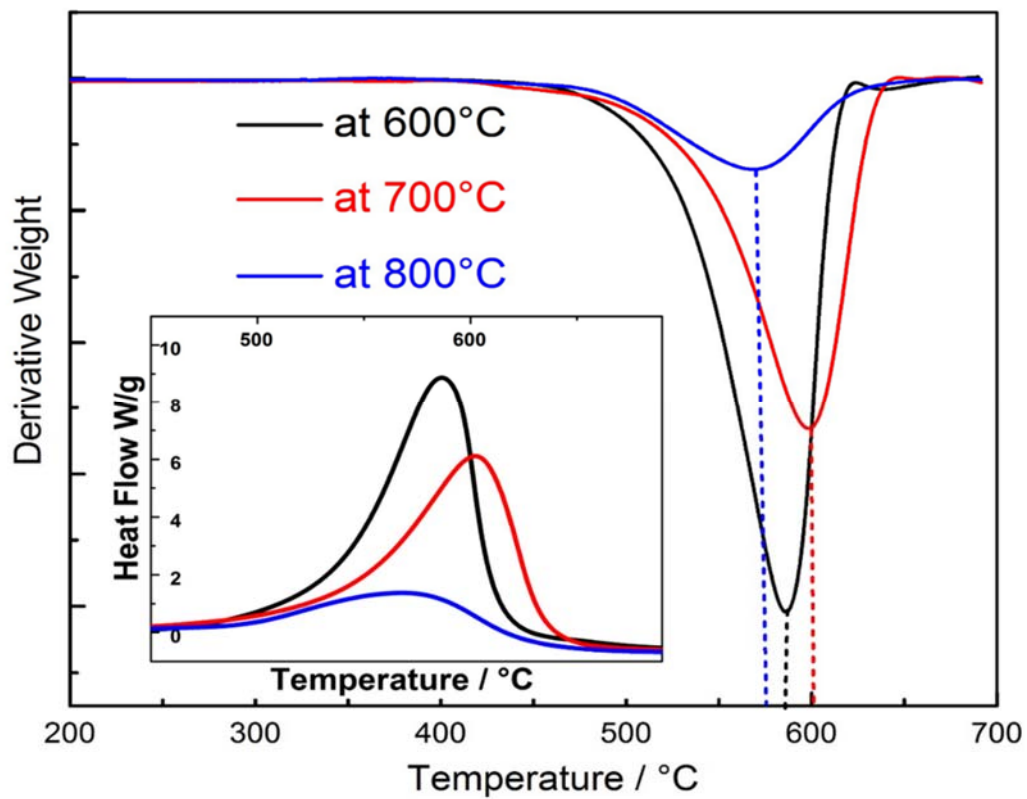
and (C) 800°C

630

631

632





633

634 Fig. 7 DTG-TPO and DSC results of the spent 0.5/ceramic at 600 °C, 700 °C, and

635

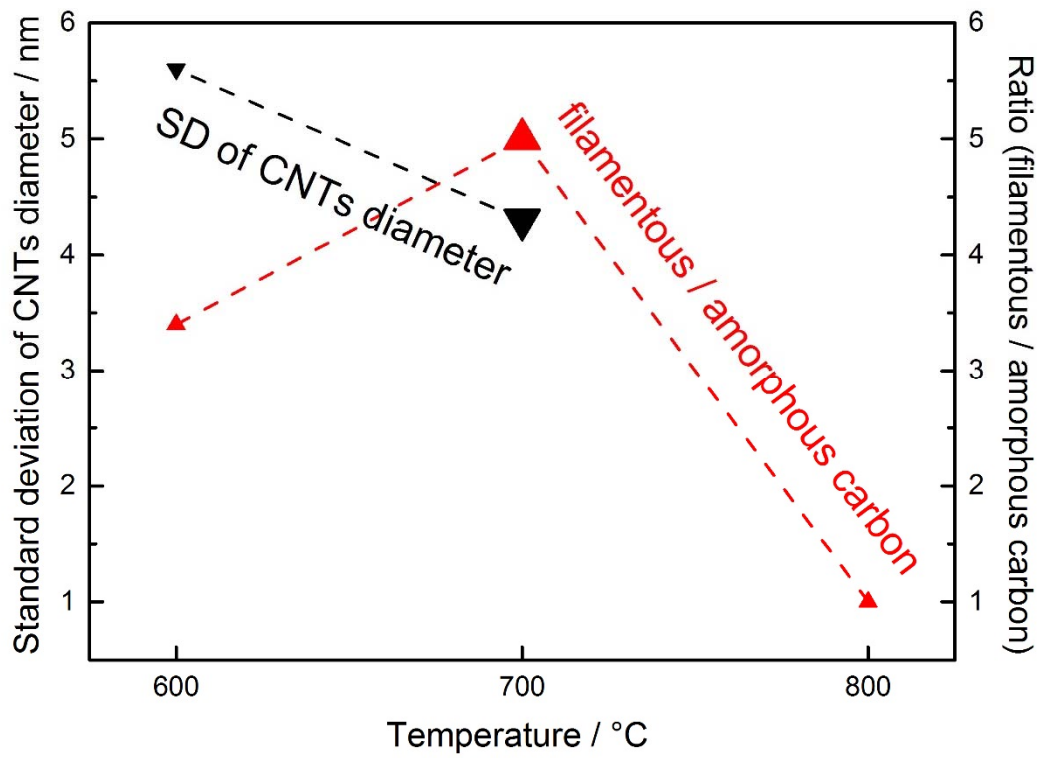
800 °C

636

637

638

639



640

641

Fig. 8 Trends of standard deviation (SD) of CNTs diameter and

642

filamentous/amorphous carbon ratio at 600 °C, 700 °C, and 800 °C

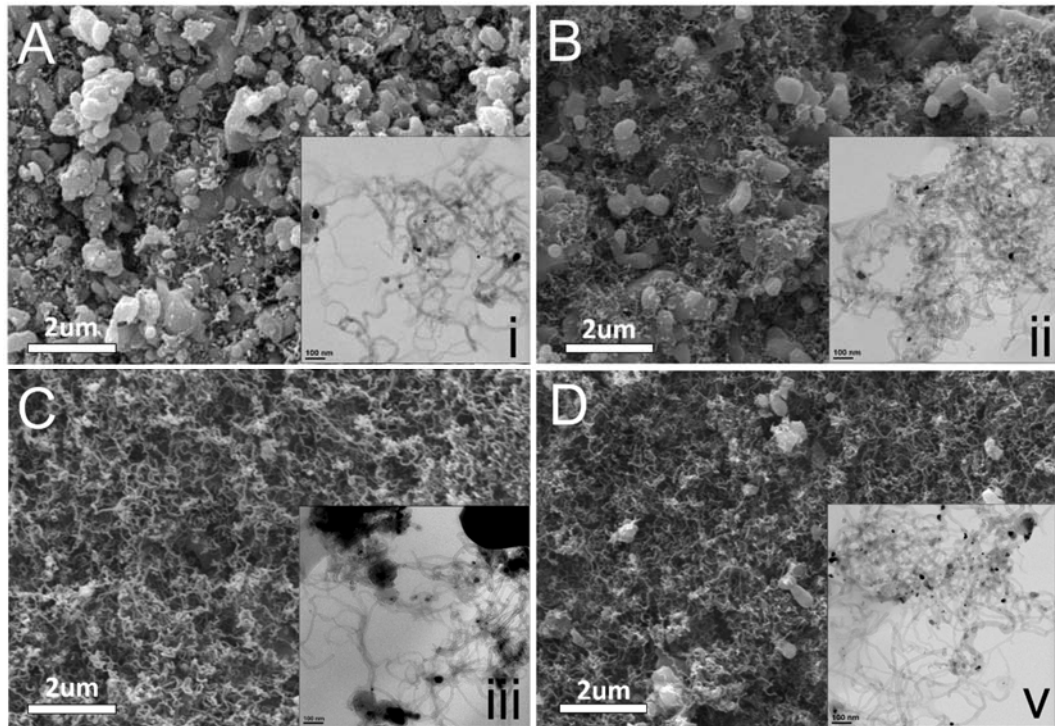
643

644

645

646

647



648

649

Fig. 9 SEM results of CNTs formation for 0.1/ceramic (A), 0.5/ceramic (B),

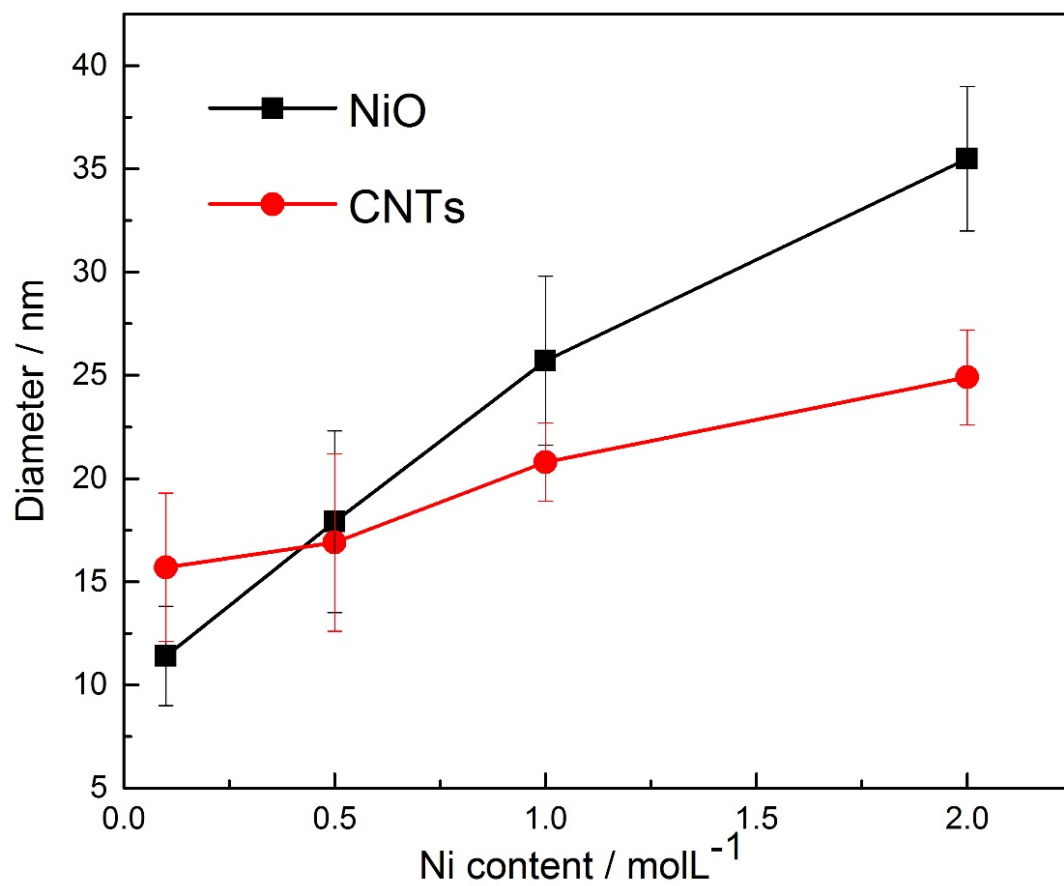
650

1.0/ceramic (C), and 2.0/ceramic (D) and corresponding TEM (i-v)

651

652

653



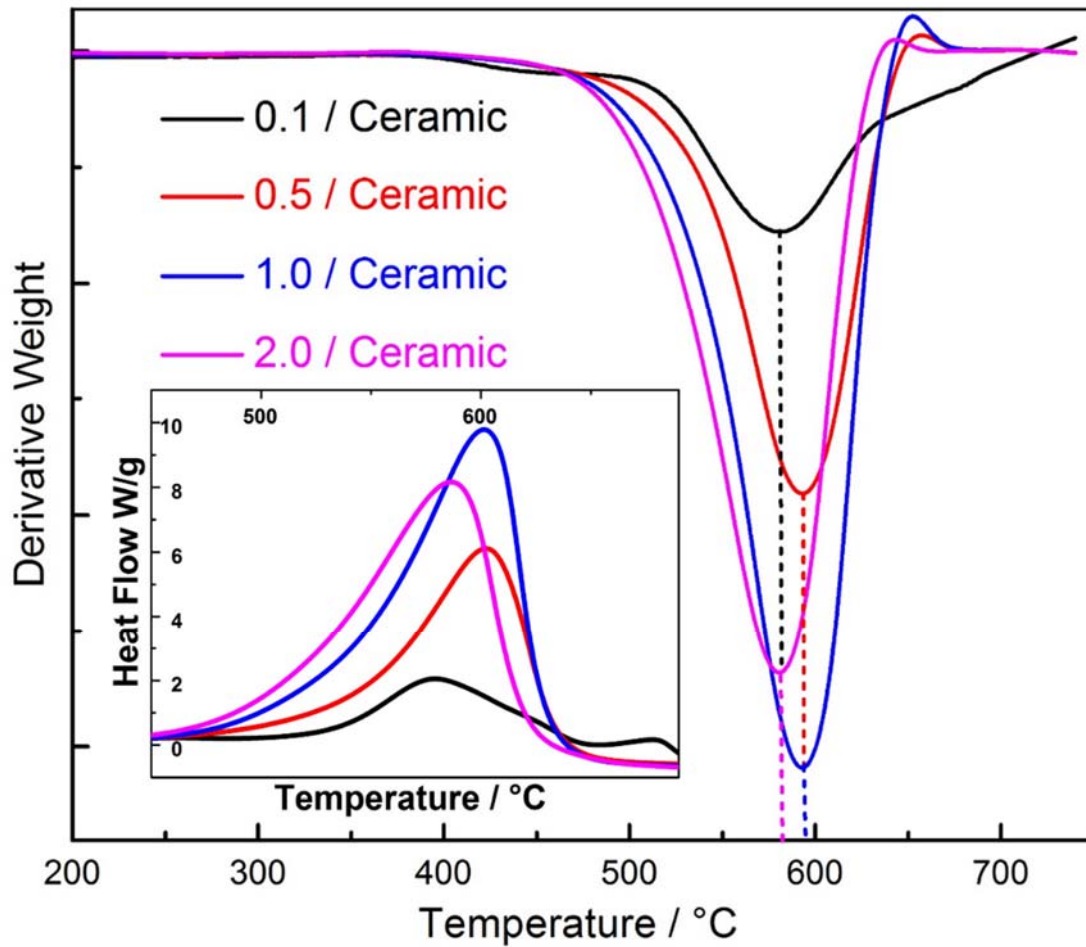
654

655 Fig. 10 Diameter distribution comparison for fresh and spent Ni/ceramic catalysts

656

657

658



659

660 Fig. 11 DTG-TPO and DSC results of the spent 0.1/ceramic, 0.5/ceramic, 1.0/ceramic

661

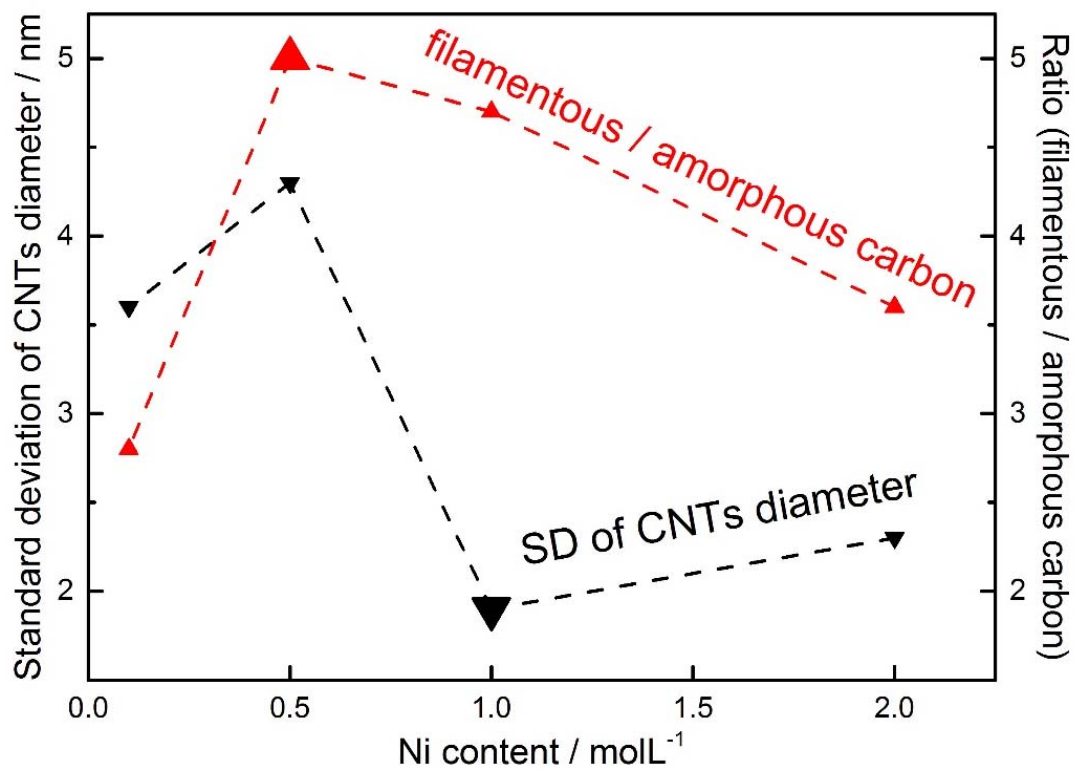
and 2.0/ceramic catalysts at 700 °C

662

663

664

665



666

667

Fig. 12 Trends of standard deviation (SD) of CNTs diameter and

668

filamentous/amorphous carbon ratio with different Ni loading ceramic catalysts

669